J Nanopart Res (2011) 13:4173–4188
DOI 10.1007/s11051-011-0362-7

RESEARCH PAPER

Synthesis, characterization, and in vitro biological evaluation of highly stable diversely functionalized superparamagnetic iron oxide nanoparticles

Dipsikha Bhattacharya · Sumanta K. Sahu · Indranil Banerjee · Manasmita Das · Debashish Mishra · Tapas K. Maiti · Panchanan Pramanik

Received: 22 December 2010 / Accepted: 27 March 2011 / Published online: 17 April 2011

Abstract In this article, we report the design and synthesis of a series of well-dispersed superparamagnetic iron oxide nanoparticles (SPIONs) using chitosan as a surface modifying agent to develop a potential T_2 contrast probe for magnetic resonance imaging (MRI). The amine, carboxyl, hydroxyl, and thiol functionalities were introduced on chitosan-coated magnetic probe via simple reactions with small reactive organic molecules to afford a series of biofunctionalized nanoparticles. Physico-chemical characterizations of these functionalized nanoparticles were performed by TEM, XRD, DLS, FTIR, and VSM. The colloidal stability of these functionalized iron oxide nanoparticles was investigated in presence of phosphate buffer saline, high salt concentrations and different cell media for 1 week. MRI analysis of human cervical carcinoma (HeLa) cell lines treated with nanoparticles elucidated that the amine-functionalized nanoparticles exhibited higher amount of signal darkening and lower T_2 relaxation in comparison to the others. The cellular internalization efficacy of these functionalized SPIONs was also investigated with HeLa cancer cell line by magnetically activated cell sorting (MACS) and fluorescence microscopy and results established selectively higher internalization efficacy of amine-functionalized nanoparticles to cancer cells. These positive attributes demonstrated that these nanoconjugates can be used as a promising platform for further in vitro and in vivo biological evaluations.

Keywords SPIONs · Chitosan · Cancer · MRI · Nanoconjugates · Colloids · Nanomedicine

D. Bhattacharya · S. K. Sahu · M. Das · P. Pramanik (✉)
Department of Chemistry, Indian Institute of Technology Kharagpur, Kharagpur 721302, India
e-mail: dipsikha.chem@gmail.com

I. Banerjee · D. Mishra · T. K. Maiti
Department of Biotechnology, Indian Institute of Technology Kharagpur, Kharagpur 721302, India

Introduction

For the past three decades, superparamagnetic iron oxide nanoparticles (SPIONs) have been established as a promising platform because of their eclectic biomedical applications such as, targeted drug delivery (Dilnawaz et al. 2010), hyperthermia (Sonvico et al. 2005), magnetic resonance imaging (MRI) contrast enhancement (Tan et al. 2010; Shi et al. 2008), magnetically mediated separation of biomolecules (Gu et al. 2006). Especially magnetic nanoparticles are receiving considerable attention because these are known as an excellent MR contrast agent for non-invasive cellular and molecular imaging (Hu et al. 2006; Weissleder et al. 2000; Veiseh et al. 2005; Hu et al. 2006; Bulte and Kraitchman 2004). Despite significant efforts made in fabricating novel magnetic

nanoparticles with T_2 contrasting ability, challenges remain in integrating colloidal suspensions of magnetite nanoparticles with good dispersibility, high biocompatibility, and superior magnetic properties for MRI application. The magnetic nanoparticles possess agglomeration tendency followed by the rapid clearance by reticuloendothelial system (RES) because of their absorption by plasma proteins due to the higher surface to volume ratio (Weissleder et al. 1995). It was recently investigated that to develop a highly stable nanoparticles with desired magnetic properties for eclectic biomedical applications, particle size, charge, and surface chemistry of these nanoparticles are of prime concern (Chithrani et al. 2006; Win and Feng 2005; Yuan et al. 2006). Meanwhile, enormous efforts have been reported in surface modification to prepare a stable suspension of nanoconjugates with extreme biocompatibility, biodegradability, and ligand conjugation ability along with T_2 negative contrast enhancement ability.

There are several reports on the surface modification of highly stable magnetic nanoparticles functionalized with poly(vinyl alcohol) (Lin et al. 2003), polyethylene glycol (Zhang et al. 2002), dextran (Shen et al. 1993), chitosan (Lee et al. 2005), poloxamers (Lin et al. 2009), etc., for diverse biomedical applications. These polymeric stabilizing agents contain reactive functional handles which not only provide sol stabilization through steric or electrostatic repulsion but also ensure high-density ligand-grafting on the nanoparticle surface for immobilization with specific biomolecules. An alternative approach incorporates the surface modification of magnetic surface with small coupling agents that ensures the availability of functional groups on magnetite in addition to sol stabilization. Organosilanes and organophosphorous couplings agents are also well-known small coupling agents but the problem involves in the modification of organosilanes is the probability of homocondensation in presence of traces of water (Smaihi et al. 2004). Organophosphorous coupling agents afford highly stable nanoparticles via developing a monolayer on the surface under physiological conditions. Recently we have established a series of phosphonic acid modified magnetic nanoparticles with different pendant groups but the use of these phosphonic acid stabilized magnetic nanoparticles as MRI contrast agents is yet unexplored (Mohapatra and Pramanik 2009). Taking the above into mind, we have designed these highly dispersible polymer modified magnetic nanoparticles intending to fabricate a magnetic probe for MRI imaging. As the literature related to the design and fabrication of functional SPIONs with various surface-pendant groups involving natural polymers are extremely sparse, we have chosen chitosan as our stabilizing polymer because of its well-established biocompatibility, in vivo biodegradability, and availability of reactive OH as well as NH_2 functional groups, which in addition to providing an anchoring site to metal-oxide surface also affords a complementary site for further chemical modifications (Li et al. 2008; Yi et al. 2005; Ravi Kumar et al. 2004). The most common procedure towards the preparation of chitosan-based magnetic colloid consists of simple, post-synthetic addition of chitosan or *o*-carboxymethyl chitosan to an aqueous dispersion of iron oxide nanoparticles with ultrasonication (Zhu et al. 2008). Alternatively, chitosan-coated magnetic nanoparticle formulation can also be synthesized via the physical adsorption of chitosan onto oleic acid stabilized magnetite nanoparticles (Kim et al. 2005). But till now there was very few reports about the surface modification of chitosan-functionalized magnetite nanoparticles as a potential probe for MRI.

To the best of our knowledge, no researchers to date have focused on a purely water-based biofuctionalizations and in vitro MRI evaluation of magnetite nanoparticles using chitosan as the polymeric modifier. Our aim is to develop a series of highly stable chitosan-coated magnetic nanoparticles with different functional groups on magnetic surface which render the nanoparticles highly hydrophilic and stable with respect to agglomeration and these functionalized nanoparticles are used as a probe for MRI. The synthetic process involves a modified two step coprecipitation of Fe^{3+} and Fe^{2+} under alkaline conditions using sodium alginate as a stabilizer (Ma et al. 2007). Subsequent modification of this modified SPIONs with chitosan imparts an amine-rich nanomagnetic support, which, following further functionalizations with small organic molecules lead to the formation of magnetite nanoparticles with surface-pendant $–NH_2$, –COOH, –OH, and –SH functional groups. These magnetic nanoparticles with reactive functionalities showed good colloidal stability in phosphate buffer saline (PBS), fetal bovine serum, and cell media (MEM), respectively. These

nanoparticles also exhibited good stability in NaCl solution (up to 1 M) and against various pHs (5–10). Cell viability assays showed that the functionalized magnetic nanoparticles have little effect on HeLa cell viability. The effect of different functionalized magnetic nanoparticles to cancer cell line was investigated by magnetically activated cell line and fluorescence microscopy and the results showed that the internalization of amine-functionalized nanoparticles was considerably higher compared to the others. The MRI studies using HeLa cancer cell line demonstrated that the amine-functionalized nanoparticles exhibited significantly higher signal darkening as well as lower T_2 relaxation values in comparison to other functionalized nanoparticles. These studies exhibited that these diversely functionalized nanoparticles can be utilized as a promising platform for MRI imaging.

Experimental

Materials

$FeCl_3$ and $FeSO_4$ were obtained from Merck, Germany. Chitosan (medium molecular weight), sodium alginate, succinic anhydride, *N*-hydroxysuccinimide (NHS), 1-[3-(dimethylamino) propyl]-3-ethylcarbodiimide hydrochloride (EDC), trinitrobenzene sulfonic acid (TNBS), 2,3 epoxy-1-propanol (glycidol), and L-cysteine were obtained from Aldrich Chemicals, USA. Commercially available *N*,*N*-dimethyl formamide (DMF) was purified by vacuum distillation. Commercially available triethylamine was purified by distillation before use.

Surface modification of Fe_3O_4 nanoparticles by the pH responsive polymer chitosan (SPION-NH_2)

Superparamagnetic magnetite nanoparticles were prepared by controlled chemical co-precipitation of Fe^{2+} and Fe^{3+} (1:2) ratio from ammoniacal solution under argon atmosphere using a desired stabilizer (Bee et al. 1995). Briefly, 278 mg of $FeSO_4{\cdot}7H_2O$ and 324 mg of $FeCl_3$ were dissolved in 50 mL of Millipore water and the resulting solution was vigorously stirred followed by the drop wise addition of about 5 mL of 25% NH_3 (1 drop per minute). Subsequently 30 mL of sodium alginate solution was dropwisely added to this suspension and the solution was heated at 80 °C with vigorous mechanical stirring for 2 h to control the growth of the nanoparticles. The obtained black product was centrifuged at 10,000 rpm for 20 min to remove the solid material and the black supernatant was collected.

For amine-functionalized magnetic nanoparticles, 100 mL of a freshly prepared dialyzed aqueous solution of chitosan (0.5 mg/mL in 100 mL Millipore water) was added to 100 mg of colloidal suspension of magnetite nanoparticles at pH 4–5 with sonication using a high intensity ultrasonic probe for an hour. The resulting suspension was then stirred vigorously on a magnetic stirrer at 60 °C for 12 h. The particles were then isolated with a rare-earth magnet, washed 3 times with deionized water and resuspended in PBS.

Synthesis of carboxyl-functionalized superparamagnetic iron oxide nanoparticles (SPION-COOH)

To a solution of 50 mg of succinic anhydride in distilled DMF, aminated nanoparticles (50 mg nanoparticles dispersed in 10 mL DMF) were added dropwise with ultrasonication. A catalytic amount of distilled triethylamine was added to the resulting suspension and the reaction was stirred in a magnetic stirrer for 24 h. The particles were finally recovered by magnetic concentration, washed with distilled water and dried using acetone.

Synthesis of hydroxyl-functionalized superparamagnetic iron oxide nanoparticles (SPION-OH)

In a typical experiment, 30 mg of amine-functionalized magnetite was dispersed in presence of 10 mL of ethanol using sonication. 5 mL of glycidol was dissolved in 10 mL of ethanol and this glycidol solution was very slowly added to the black suspension of magnetite during sonication for more than 30 min. This solution was stirred in a magnetic stirrer for 12 h and separated after repetitive washing with ethanol on a magnet.

Synthesis of thiol-functionalized superparamagnetic iron oxide nanoparticles (SPION-SH)

In a typical experiment, 30 mg L-cysteine was dissolved in 15 mL of Millipore water followed by the addition of 30 mg of EDC and 30 mg of NHS maintaining the solution pH at 5 under sonication. This solution was stirred for almost 2 h. 30 mg of aminated magnetite was dispersed in 10 mL of water using ultrasonication and this magnetite suspension was added dropwisely to the solution of L-cysteine and this solution was stirred for 12 h and separated after repetitive washing with milipure water on a magnet.

Characterization

The determination of amino groups on the surface of chitosan-functionalized magnetite nanoparticles was performed using the 2,4,6-trinitrobenzenesulfonic acid (TNBS) method (Levy et al. 1993). This procedure consisted of the incubation of the material with an excess of TNBS and the back-titration of the unreacted amount of the reagent. The conversion of amine groups on the nanoparticle surface into carboxyl, hydroxyl, and thiol groups were also quantified by determining the residual amino group concentration by TNBS assay. XRD (X'pert Pro Phillips X-ray diffractometer) was performed to identify the structure of the bare-SPION and SPION-NH_2 using Co Kα radiation ($\lambda = 1.74$ Å) between 20° and 90° (2θ) at 27 °C. The size and morphology of Fe_3O_4 nanoparticles in the SPION-NH_2, SPION-COOH, SPION-OH, and SPION-SH were observed by TEM (JEOL 3010, Japan). The hydrodynamic (HD) size of the particle aggregates was measured by laser light scattering using a Brookhaven 90 Plus particle size analyzer. The surface charge of the nanoparticles was investigated through ξ potential measurements (Zetasizer 4, Malvern Instruments, UK). The successful synthesis of amine-, carboxyl-, hydroxyl-, and thiol-functionalized nanoparticles were studied by Fourier Transform Infrared (FTIR) spectroscopy using a Thermo Nicolet Nexux FTIR model 870 spectrometer. For cell culture experiment, the cells cultivated for in vitro experiments were human cervix adenocarcinoma, HeLa and human osteosarcoma, obtained from the National Centre for Cell Sciences (NCCS), Pune, India. All cell lines were cultured on minimum essential medium (MEM) with 10% fetal calf serum, 100 units mL^{-1} penicillin, 100 μg mL^{-1} streptomycin, 4 mM L-glutamine at 37 °C in a 5% CO_2 and 95% air humidified atmosphere. For in vitro cell viability assay, 4×10^5 HeLa cells were seeded into 96-well tissue culture plates in a total volume of 180 μL of complete media and kept for 18 h. After that 20 μL of different nanoparticle preparations were added to the cells at different concentrations (50, 100, 150, and 200 μg mL^{-1}), incubated for 4 h at 37 °C in a humidified incubator (HERA cell) maintained at 5% CO_2, and the cell viability was assessed by the 3-(4,5-dimethylthiazol)-2-diphenyltertrazolium bromide (MTT) test. The effect of surface coating on the uptake of nanoparticles by HeLa cells was evaluated by magnetically activated cell sorting (MACS) method. For that purpose, four different sets in triplicate each containing 5×10^5 cells were incubated with different nanoparticle preparations (100 μg/mL) in the culture medium (MEM, 10% FBS) at 37 °C in humidified 5% CO_2 incubator. After 4 h of incubation, the cells were washed with PBS to remove free nanoparticles and cell sorting was performed with MACS. Three replicates were measured and the results were expressed as mean ± SD (SD means standard deviation). For fluorescence imaging, HeLa cells were treated with different nanoparticle preparations (1 mg mL^{-1}) followed by incubation for 24 h. After that, these cells were smeared on a clean glass slide, fixed with 3.7% formaldehyde for 15 min, permeabilized with 0.1% Triton X-100, and stained with DAPI (1 mg mL^{-1}) for 5 min at 37 °C. The cells were then washed with PBS and examined by fluorescence microscopy (Olympus IX 70). For the determination of iron content present in these nanoparticles, the iron present in the nanoparticle was completely extracted by dissolving the nanoparticles (10 mg) in HCl (10 mL, 30% v/v) for 2 h at 50–60 °C. Ammonium persulfate (1.0 mg) was then added to oxidize the ferrous ions present in the above solution to ferric ions. Potassium thiocyanate (1 mL, 0.1 M) was added to this solution to form a blood-red iron thiocyanate complex. The iron concentration was determined by spectrophotometric measurements at 478 nm using a Shimadzu UV-1700 spectrophotometer. Samples for MR phantom imaging were

prepared by suspending 10^6 cells in low-melting 1% agarose gel (50 μL). Cell suspensions cultured with different nanoparticle concentrations (0.01–0.05 mg mL^{-1}) were loaded into 1.5 mL eppendorf tubes and allowed to solidify at 4 °C. Samples were then sealed with additional agarose to avoid air susceptibility artifacts. MRI was performed with a 1.5 T clinical MRI scanner (GE Medical systems, Milwaukee) using a prefabricated sample holder. A spin-echo multisection pulse sequence was selected from the GE Medical systems to acquire MR phantom images. A repetition time (TR) of 2100 ms and variable echo times (TE) of 42–110 ms were used. The spatial resolution parameters were set as follows: an acquisition matrix of 256 × 256, field of view of 240 × 240 mm^2, section thickness of 8 mm, and two averages. The MRI signal intensity (SI) was measured using the in-built software. T_2 values were obtained by plotting the SI of each sample over a range of TE values. T_2 relaxation times were then calculated by fitting a first-order exponential decay curve to the plot. The fitting equation can be expressed as $SI = Ae_E^{-T}/_2^T + B$, where A is the amplitude and B is the offset.

Results and discussions

Synthesis of functionalized magnetite nanoparticles with surface-pendant amine, carboxyl, hydroxyl, and thiol groups

For the successful biofunctionalizations of SPIONs, a modified two-step co-precipitation was executed in alkaline conditions followed by the addition of sodium alginate which plays the role of growth controlling agent of magnetic nanocrystals (Nath et al. 2009; Ma et al. 2007). These alginate-stabilized magnetite nanoparticles were further modified with chitosan, an amine-rich natural polymer to impart active amine functionalities on the nanoparticulate system. It was assumed that the reason for the stability of this Alg-SPION was the governing process of chemisorptions between terminal carboxyl group of alginate to the Fe site of the Fe–OH particles depending on the steric necessity and the curvature of the surface (Nath et al. 2009). As sodium alginate acts as a stabilizing as well as a growth-preventing agent during nanoparticle precipitation, deposition of the layer of polyelectrolyte chitosan on alginate–magnetite provides steric as well as electrostatic stabilization to the sol, in addition to providing a reactive, chemically modifiable, primary amine handle, amenable to conjugation with a variety of functional molecules through sulfhydryl, carboxyl, and imine chemistry (Das et al. 2008). Even there is a possibility that the protonated amine functions of chitosan partially binding to some of the free surface-exposed carboxylate functions of alginate; however, because of the polycationic nature of the polymer, not all the amine functions are involved in electrostatic binding with the anioinic surface of alginate–magnetite. A part of these functional amine groups still remain surface-exposed thereby imparting a positive charge to these magneto polymeric particles in the lower pH range.

The primary amine groups of these chitosan-coated magnetite nanoparticles (SPION-NH_2) were further interchanged with carboxyl, hydroxyl, and thiol groups using diverse conjugation strategies, as elaborated in Scheme 1. Carboxylic acid (–CO_2H) groups were introduced onto this magnetic support by a simple ring opening linker elongation reaction with succinic anhydride to impart SPION-COOH nanoparticles. Glycidylation was undertaken to convert the primary amine termini on the nanoparticle surface to free hydroxyl groups. Thiol-functionalized magnetic nanoparticles were prepared by the conjugation of –COOH groups of L-cysteine with the reactive amine functionalities of chitosan. The carboxyl groups of L-cysteine was activated by the simple EDC/NHS at pH 5 followed by the reaction with –NH_2 groups of chitosan (Schnürch et al. 2000).

Surface chemistry: FTIR studies

The FTIR spectra of the as-prepared SPIONs have been depicted in Figs. 1A–C and 2A, B, respectively. In the FTIR spectrum of Alg-SPION, the bands corresponding to the asymmetric stretching and symmetric stretching of –COO^- were observed at 1620 and 1410 cm^{-1}; the blue shift, however, may be attributed to a partial back-bonding of –COO^- to the iron(III) center of magnetite (Ma et al. 2007). It can be anticipated from the shifting of –Fe–O band to higher frequency region that the COO^- terminal of alginate coordinates to the Fe^{3+} center of the iron oxide core and the hypothesis is well-supported by

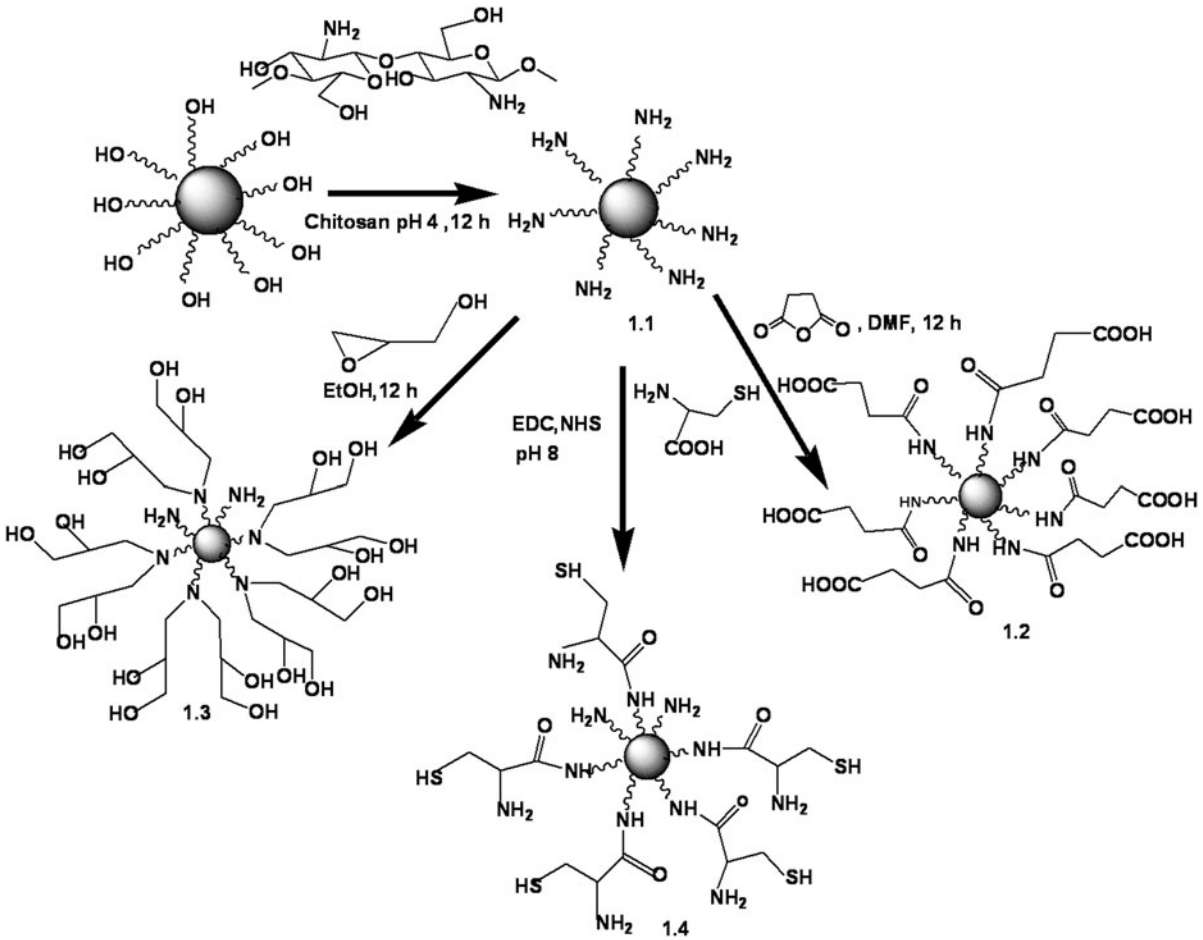

Scheme 1 Synthesis of amine-, carboxyl-, hydroxyl-, and thiol-functionalized iron oxide nanoparticles by the simple reaction with small functional organic molecules

the results of Kawaguchi et al. (2001). In the FTIR spectrum of SPION-NH_2, the –N–H bending vibration at 1596 cm^{-1} shifted to 1637 cm^{-1} (Chang and Chen 2005), the 1384 cm^{-1} peak of –C–O bending vibration shifted to 1398 cm^{-1} and additional signals for –Fe–O and –Fe–O–C stretching vibration appeared at 624 cm^{-1} (Chen et al. 2008), corroborating to the presence of a polymeric chitosan-layer on the surface of iron oxide. A broad band in the range of 1080–1034 cm^{-1} accounted for the –Fe–O–C stretching vibration. In addition, a broad band could be visualized in the range of 3300–3400 cm^{-1}, indicative of the presence of –NH_2 and –OH groups on the nanoparticle surface. The bands at 1075 and 1033 cm^{-1}, characteristic of the saccharine structure, are due to skeletal vibrations involving C–O stretching. Surface treatment of these aminated nanoparticles with succinic anhydride interchanged the amine groups on SPION-NH_2 with carboxyl groups. Increased absorbance was observed at 1656 cm^{-1} (Amide I), 1560–1640 cm^{-1} (Amide II), and 1426 cm^{-1} (Amide III), respectively, indicating successful transformation of the free primary amine functions of SPION-NH_2 to –NH–CO– groups. Although somewhat weakly intense, the typical vibrations of –CO_2H group (1736 cm^{-1}) appeared in the corresponding spectrum, which evidences the successful derivation of the surface amino groups with succinic anhydride.

In the hydroxyl decorated magnetite nanoparticles (SPION-OH), the peaks at 3400–3600 cm^{-1} was intensified and peak appeared at 1633 cm^{-1} clearly

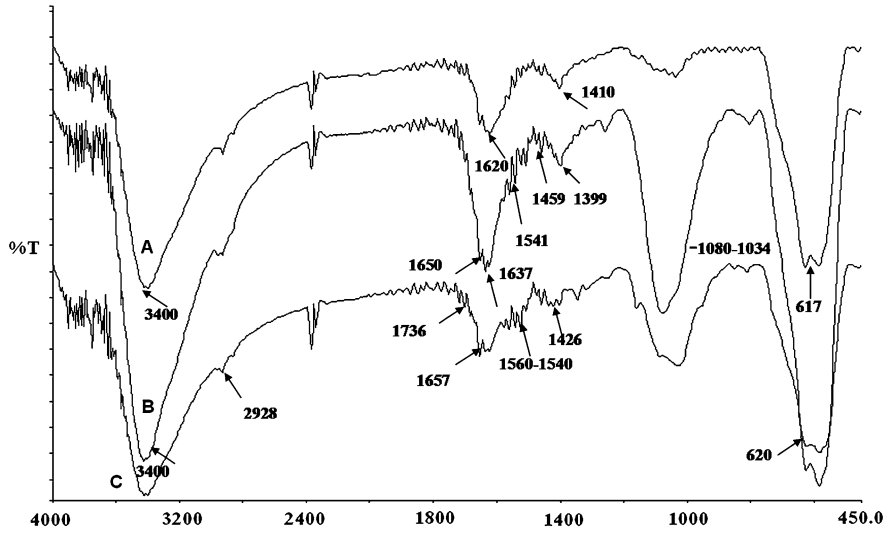

Fig. 1 FTIR spectra of (*A*) Alg-SPION, (*B*) SPION-NH_2, (*C*) SPION-COOH

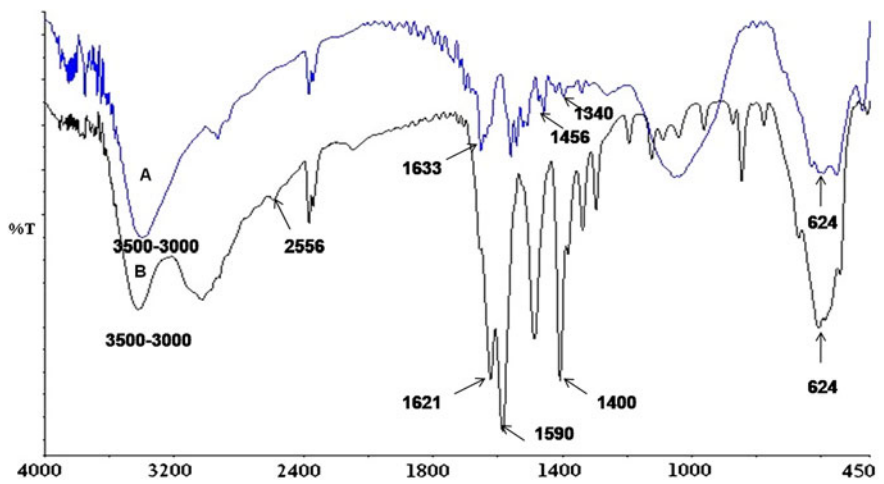

Fig. 2 FTIR spectra of (*A*) SPION-OH and (*B*) SPION-SH

indicates the extent of some amount of amine groups on the surface of SPION-OHs. The peaks appeared at 1456 and 1340 cm^{-1} clearly attributes to the scissoring and twisting vibrations of $–CH_2–O–CH_2$ modes, respectively (Wang et al. 2008). In the L-cysteine functionalized chitosan-coated magnetite nanoparticles (SPION-SH), a band at 1621 cm^{-1} associated with –CO stretching vibration testified to the successful modification of magnetite surface by primary amine groups and 1590 cm^{-1}, 1400 cm^{-1} (Amide III) increase due to the presence of amide bond between the L-cysteine moiety and SPION-NH_2. Another sharp peak was observed at 2550 cm^{-1} due to the presence of –SH present on the surface of cysteine-functionalized SPION-NH_2 (Aryal et al. 2006).

Quantification of amino, carboxyl, aldehyde, hydroxyl, and thiol groups on the nanoparticle surface

The TNBS method was used to determine the number of amine groups present on the surface of chitosan-stabilized magnetite nanoparticles. The number of carboxyl, hydroxyl, and thiol groups on the surface of these functionalized nanoparticles were also quantified using the same method by determination of residual amine concentration on the surface of magnetite nanoparticles. The amine density on the surface of SPION-NH_2 was estimated as 3.25 μmol/mg by standard TNBS method and it was given in Table 1. From the results of the TNBS assay, it is clear that the amine grafting density on the

Table 1 Concentration and the numbers of amino, carboxyl and hydroxyl and thiol groups present on the nanoparticle surface

SPION modification	Functional end groups	Surface amine density (μmol/g)	Concentration of functionalized groups	Number of functionalized groups
Amine	$–NH_2$	3.25	3.25	180
Carboxyl	–COOH	0.25	3.01	166
Hydroxyl	–OH	0.28	2.98	164
Thiol	–SH	0.31	2.95	162

nanoparticle surface was considerably higher and subsequent conversion of these primary amine groups into carboxyl, hydroxyl, and thiol groups was nearly quantitative.

Crystal structure, size, and morphology of nanoparticles

The high resolution X-ray diffraction patterns of bare-SPION and chitosan-coated SPION (SPION-NH_2) have been shown in Fig. 3. The d values correspond to those of inverse spinel phase magnetite (Fe_3O_4). Six characteristics peaks for bare-SPION and SPION-NH_2 were marked by their indices (220), (311), (400), (422), (511), (440) and were observed in this sample. These peaks are consistent with database with (JCPDS card no. 77-1545) and revealed that resultant nanoparticles are inverse spinel in structure. Broadening of the diffraction bands is indicative of nanocrystalline nature of the synthesized powder. Crystallite size was evaluated from the XRD data using Debye–Scherrer equation, $d = K\lambda/\beta\cos\theta$, where, d is the crystal thickness, K is Debye–Scherrer constant (0.89), λ is the X-ray wavelength (Co = 1.789 Å). The mean crystallite size was calculated to be around 10 nm.

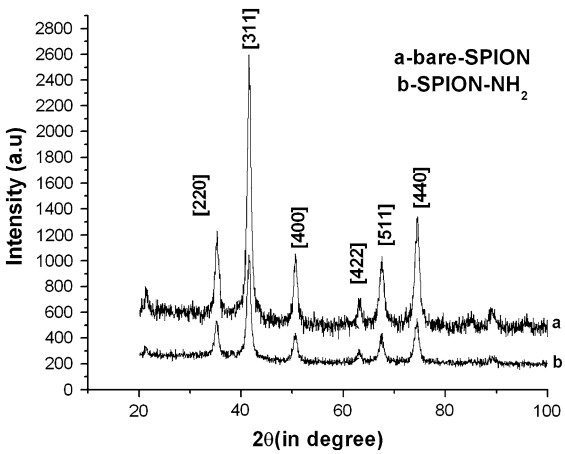

Fig. 3 X-ray diffraction pattern of superparamagnetic bare magnetite and chitosan-stabilized magnetite nanopowder

The morphology and size of the SPION-NH_2, SPION-COOH, SPION-OH, and SPION-SH were investigated by TEM at physiological pH (Fig. 4a–d). It was observed that all these functionalized magnetic nanoparticles were quasispherical and with an average diameter of 16.5, 15.6, 16.2, and 16.7 nm, respectively. The particle sizes were calculated by image J software. It was observed that the sizes of nanoparticles calculated from the XRD data using the Scherrer equation were well matched with those obtained from the sizes obtained from the TEM micrographs.

Colloidal stability of magnetite nanoparticles under physiological conditions

Colloidal stability of nanoparticles under physiological conditions is known as one of the most important issues relating to the biomedical applications of nanomaterials as MR probes. The colloidal stability of these surface functionalized nanoparticles was observed for a wide range of pHs in PBS and in varied concentrations of NaCl. The colloidal stability of these nanoparticles was evaluated by measuring their hydrodynamic sizes (DLS) and zeta potentials for 1 week. The pH dependence of hydrodynamic sizes and zeta potential values of magnetic nanoparticles was observed in Fig. 5a and b which exhibited that the change of hydrodynamic sizes with respect to pH depends on the charge and surface functionalities of nanoparticles. At low pH in 0.01 M phosphate buffer, the electrostatic repulsion between the positively ($–NH_3^+$) charged SPION-NH_2s (Scheme 1) obstruct the probability of intermolecular hydrogen binding and leads to a stable suspension of SPION-NH_2 at pH 4 and showed a higher value of positive zeta potential and lower HD size of 65 nm. With

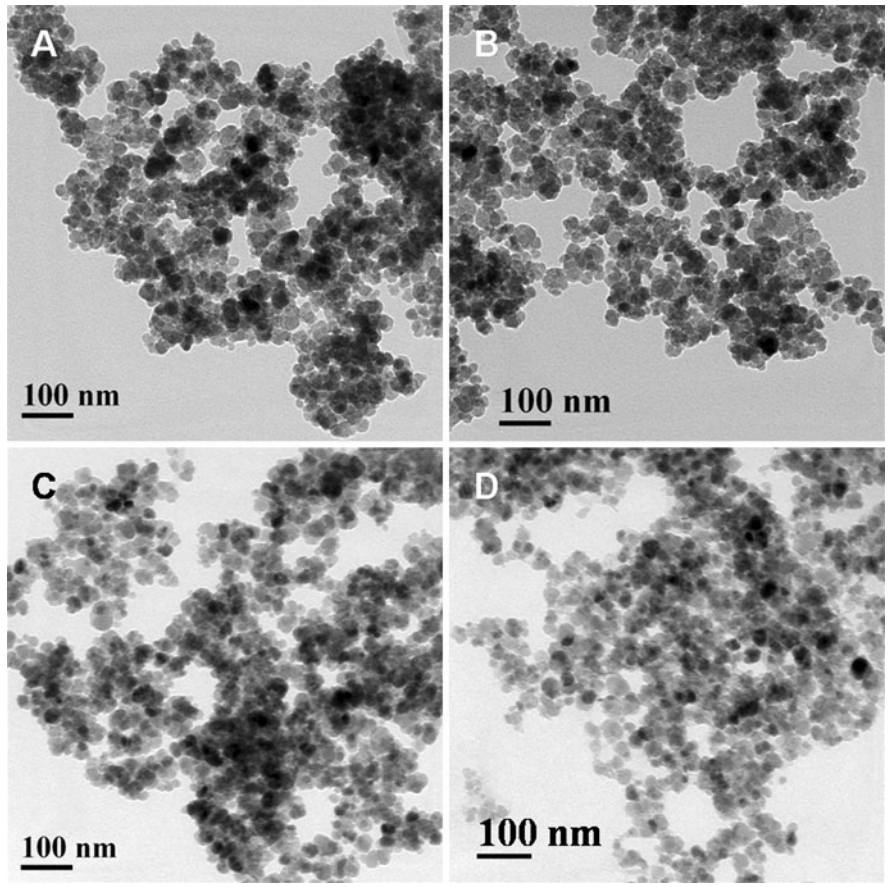

Fig. 4 TEM micrographs of **a** SPION-NH_2, **b** SPION-COOH, **c** SPION-OH, **d** SPION-SH

increasing pH, chitosan-functionalized SPIONs is susceptible to agglomeration due to the tendency of strong intermolecular hydrogen bonding between the surface coating agent chitosan (Zhu et al. 2008), reflecting a decrease in the positive zeta potential value as well as increase in HD sizes. For the SPION-COOH, the HD size observed was 95 nm at physiological pH which was considerably low from the HD sizes of SPION-NH_2 of 122 nm because of the possibility of hydrogen bonding between the surface-exposed amine groups at higher range of pH. The zeta potential of SPION-COOH became increasingly negative with increasing pH with lowering of HD value, which is pretty consistent with successive deprotonation of the carboxyl functions with concomitant pH hike. The HD sizes of SPION-OH showed stability in higher range of pH due to the possibility of hydrogen bonding between hydroxyl groups in lower range of pH. It has been thoroughly studied that the functionalization of magnetic nanoparticles with cysteine can be done only under acidic conditions (in the range of pH 4–5) because of the available free thiol groups on the surface has a tendency towards the formation of negative thiolate anions (S^-), amenable to ready oxidation and formation of intra and intermolecular disulfide linkage (Kast and Schnürch 2001; Schnürch et al. 2004). In the lower pH range of 4–5, SPION-SH possesses positive charge which might cause an elevation in the p*K*a value of the thiol moieties and a decreased amount of reactive thiolate anions on the magnetite surface. As pH rises, the hydrodynamic size of the particles increase, attributed aggregation tendency due the availability of free thiolate anions on the surface (Yin et al. 2009).

Furthermore, the effect of ionic strength on the colloidal stability of these functionalized nanoparticles was also checked in 0–1 M NaCl solutions. It was also observed in Fig. 5c that these functionalized nanoparticles were extremely stable with salt concentration as high as 1 M NaCl. This was expected due to the presence of a thick double polymeric layer

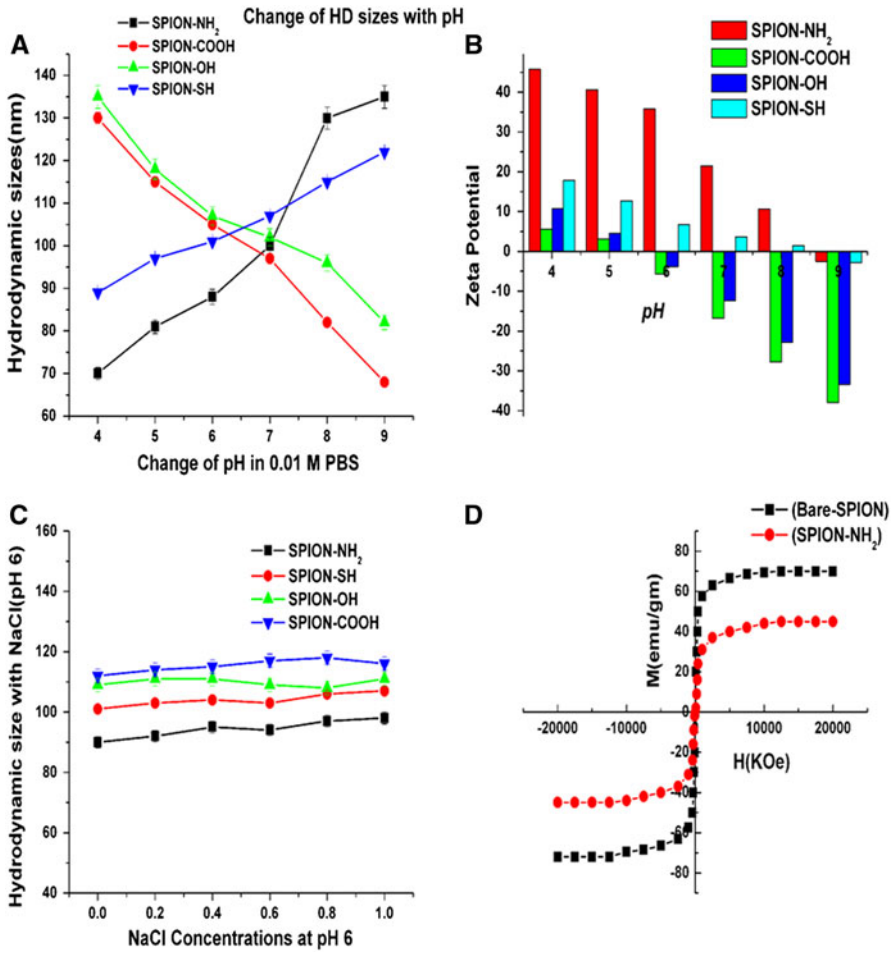

Fig. 5 **a** Variation of particle sizes of nanoconjugates against pH in 0.01 M PBS. **b** Variation of zeta potential of nanoconjugates against pH. **c** Effect of NaCl concentration (0.01–1 M) on the HD sizes of functionalized magnetite nanoparticles at pH 6. **d** Magnetization curve of both bare-SPION and SPION-NH_2 at 300 K

on the surface of magnetite nanoparticles which offsets the attraction between the magnetite particles during agglomeration (Marco et al. 2007; Flory 1953).

Time-dependent variation in hydrodynamic sizes of these functionalized nanoparticles was measured for 7 days both in PBS and in cell culture media (containing 10% FBS) and the resulting suspensions remained non-aggregated for 7 days (Hong et al. 2008; Huang et al. 2009). Although the stability of the as-prepared MNPs in biological media is lower in comparison to PBS (pH 7.4), the HD values of these functionalized nanoparticles in different media remains nearly unchanged for more than 7 days, which ensured the desired stealthiness of the as-prepared SPIONs in the physiological condition. The hydrodynamic sizes and zeta potential values for these functionalized nanoparticles measured in both in PBS and in cell media with 10% serum (7.4) were given in Fig. 6a–d. The zeta potential values for these functionalized nanoparticles in cell media with serum were more or less compatible with the zeta potential measured in presence of PBS after 7 days from the day of preparation. As there was no such changes reflected in the zeta potential and the hydrodynamic sizes of these nanoconjugates with time for both in PBS and in cell media containing serum, so it can be inferred that our as-synthesized nanoparticles showed excellent stability and biocompatibility in presence of cell medium for 7 days, i.e., it did not adsorb a significant amount of plasma proteins from the cell culture medium.

Magnetic properties

The magnetic properties of the bare-SPION and SPION-NH_2 were characterized by vibrating sample magnetometry (VSM) and have been depicted in Fig. 5d, respectively. Anhysteric *M–H* curve without

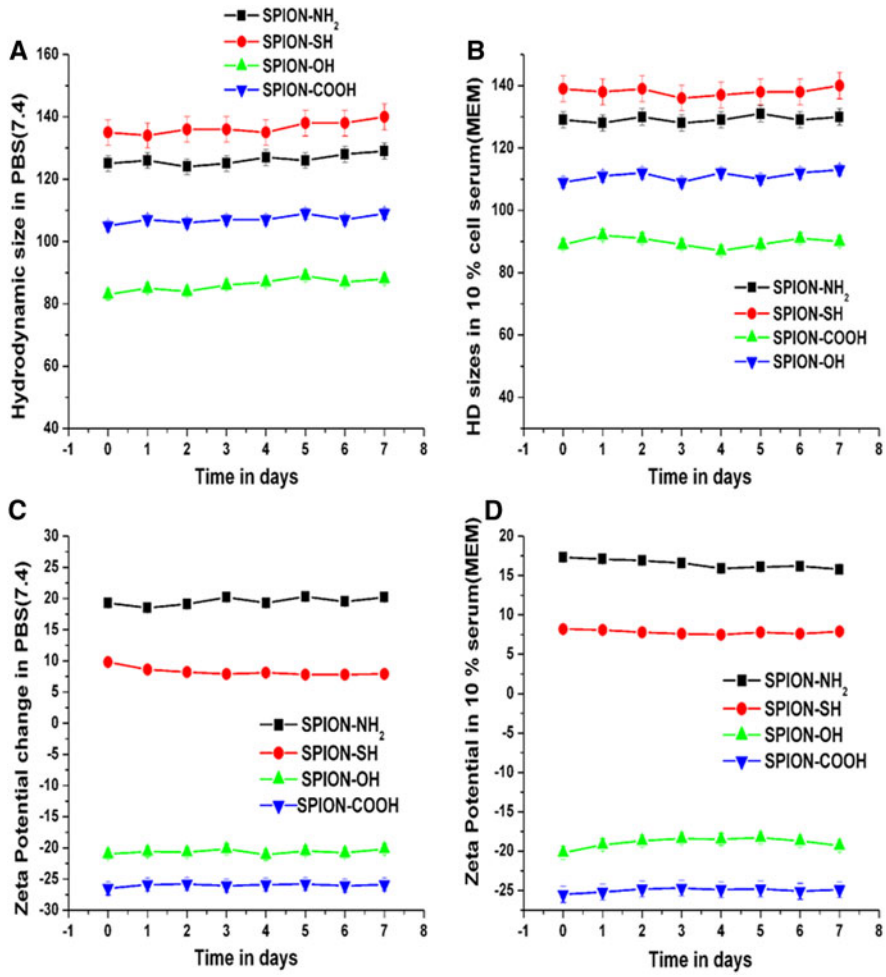

Fig. 6 **a** HD size change of functionalized nanoparticles with time in presence of PBS (7.4). **b** HD size change of functionalized nanoparticles with time in presence of DMEM media with 10% serum. **c** Zeta potential change of functionalized nanoparticles with time in presence of PBS (7.4). **d** Zeta potential change of functionalized nanoparticles with time in presence of DMEM media with 10% serum

any detectable coercivity and remanence clearly confirms that these samples are superparamagnetic in nature. The saturation magnetization of bare magnetite was found to be 72.5 emu/g, which is approximately 77% of the value possessed by bulk magnetite. This decrease in M_s value might be due to the decrease of particle size accompanied by an increase in surface area, and is consistent with our previously reported result (Das et al. 2008). Following conjugation with chitosan, a further loss of value is observed which can be attributed to the presence of nonmagnetic organic components on the nanoparticle surface.

Magnetorelaxometric studies

To evaluate these functionalized nanoparticles as MR contrast agents, the colloidal stability of amine-functionalized magnetite nanoparticles in PBS (pH 7.4) was investigated at different Fe concentrations by observing the magnetorelaxometric images of these nanoparticles on a 1.5 T small animal MR scanner. The aqueous solutions of as prepared nanoparticles were suspended in agarose with different Fe concentrations and it was observed in Fig. 7 that the T_2 weighted images decreased drastically in signal intensity with increasing concentrations of amine-functionalized nanoparticles (Jun et al. 2008). The MR phantom images darkened with increasing concentration of Fe indicating that these iron oxide nanoparticles could be used as a potential T_2 contrast agents.

Biocompatibility, intracellular uptake, and MRI studies

To examine the biocompatibility of these functionalized nanoparticles, an MTT assay was performed on

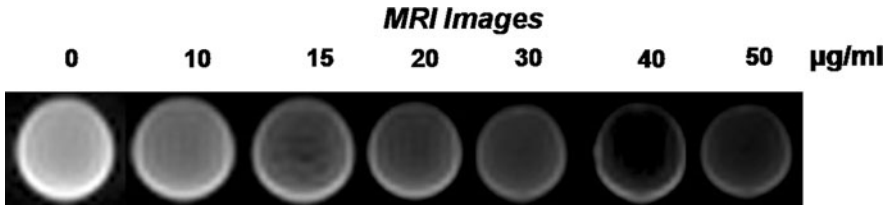

Fig. 7 T_2 weighted phantom images of amine-functionalized nanoparticles (SPION-NH_2) with different Fe concentrations

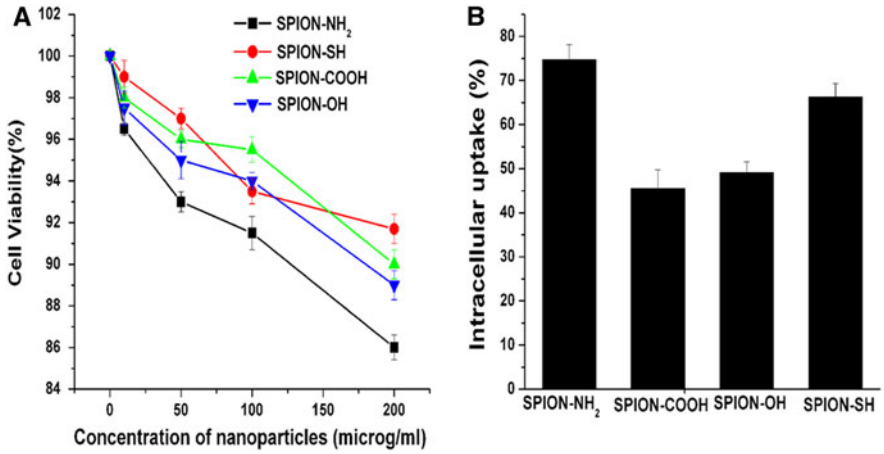

Fig. 8 **a** Effect of functionalized nanoparticles on the viability of HeLa cells. **b** Intracellular uptake of chitosan-functionalized nanoparticles and its counterpartys (after 4 h incubation) as quantified by magnetically activated cell sorting (MACS)

the human cervical HeLa cancer cell line after incubating cells with various concentrations of nanoparticles up to 200 μg/mL. After 4 h incubation, no significant reduction in cell viability was observed in Fig. 8a and the survival rate was greater than 84% even at very higher concentration of nanoparticles. Hence these nanoparticles can be used for biomedical purposes.

The intracellular uptake of our polymer-functionalized magnetite nanoparticles in HeLa cancer cell line was preliminarily assessed using magnetically activated cell sorting after 4 h and the data was presented in Fig. 8b. It was found that the positively charged SPION-NH_2 and SPION-SH demonstrated a significant amount of uptake compared to the negatively charged SPION-COOH and SPION-OH after 4 h. While significant nanoparticle internalization was observed for SPION-NH_2 after 4 h of nanoparticle incubation in the culture medium, the uptake was nominal in the case of comparatively less compared to the carboxyl- and hydroxyl-functionalized nanoparticles. As there was no confirmed plasma protein adsorption from the cell medium, it was believed that the nanoparticle internalization of SPION-NH_2 was facilitated by their positively charged surface, not via their plasma protein adsorption as reported by Chen et al. (Huang et al. 2009; Petri-Fink et al. 2008). The findings are very consistent with some earlier reports, which established that cationic modification of SPIONs significantly improves the hydrophilicity and biocompatibility of the magnetic nanosystem, while minimizing non-specific uptake by macrophages (Das et al. 2010; Petri-Fink et al. 2008).

To authenticate the above findings, the MR images of the cancer cells were subsequently taken using a with a clinical 1.5 T MRI scanner by suspending the functionalized nanoparticles treated HeLa cells in agarose. The concentrations of cultured HeLa cells were incubated with 0.05 mg Fe mL^{-1} of the as-prepared nanoparticles for 0, 1, 2, and 4 h. The T_2 weighed MR phantom images of SPION-NH_2 given in Fig. 9 exhibited a comparatively higher signal darkening for HeLa cell lines as early as 2 h, while the darkening of the images was lowest in case of SPION-OH. The signal intensity and corresponding T_2 relaxation of these HeLa cell treated functionalized nanoparticles were observed with respect to various time intervals (0–4 h) and results given in Fig. 10a, b demonstrated that the Signal intensity and corresponding T_2 relaxation value of SPION-NH_2 was considerably lower in comparison to its

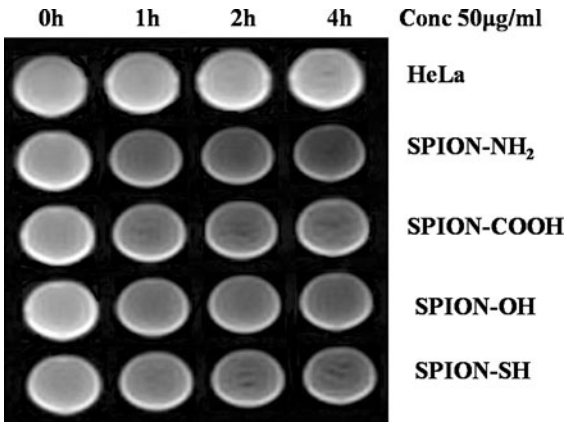

Fig. 9 Time dependent analysis of T_2-weighted spin-echo MR phantom images of HeLa cells treated with functionalized nanoparticles for 0–4 h

counterparts. These clearly confirm that the amine-functionalized nanoparticles showed higher amount of cellular internalization which was expected to be governed by cationic charge of the SPION-NH_2. Introduction of a cationic layer of chitosan on the top of the iron oxide nanoparticles not only improves their solubility in physiological buffers but also enhances their loading capacity into the cells, presumably via the negatively charged biomolecules on the cell membrane indicating passive targeting of these functionalized nanoparticles to cancer cell lines.

To further confirm the nanoparticles internalization to cancer cell lines by passive targeting, the fluorescence images of these functionalized nanoparticles were observed after 4 h of incubation at 0.05 mg Fe/mL concentration to cancer cell lines. It was clearly observed from the fluorescence images in Fig. 11 that the amine-functionalized nanoparticles showed a significantly higher uptake of nanoparticles to cancer cells compared to the other ones, indicating charge mediated endocytosis of these nanoparticles to cancer cell lines. These data matched well with the MACS studies and the cellular MRI images.

Conclusions

In a nutshell, a series of highly biocompatible and water-dispersible chitosan-functionalized superparamagnetic iron oxide nanoparticles with excellent colloidal stability and biocompatibility have been designed by a modified two-step co-precipitation approach. Diverse functional handles were introduced on the surface of magnetite nanoparticles by modifying the available, free amine groups of chitosan with a series of small organic molecules. From spectroscopic studies, it was, however, confirmed that the surface of SPION-NH_2 was functionalized with –COOH, –OH, and –SH groups. The presence of functional groups on the surface of magnetic nanoparticles exhibited good colloidal stability and the size, surface charge, and colloidal stability of the as-made SPIONs in presence of PBS, NaCl, and serum were extensively characterized using TEM, DLS, and zeta potential analysis. As smart MR contrast agents, these functionalized nanoparticles demonstrated both excellent biocompatibility and detection of MRI by

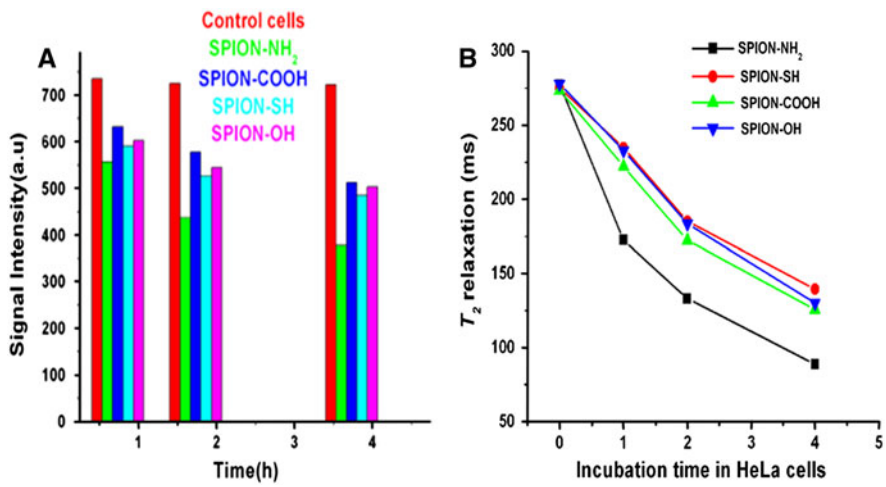

Fig. 10 **a** Effect of Signal Intensity of HeLa cell treated functionalized nanoparticles with variation in incubation time. **b** T_2 relaxation analysis of HeLa cell suspensions labeled with nanoparticles with variation in incubation time

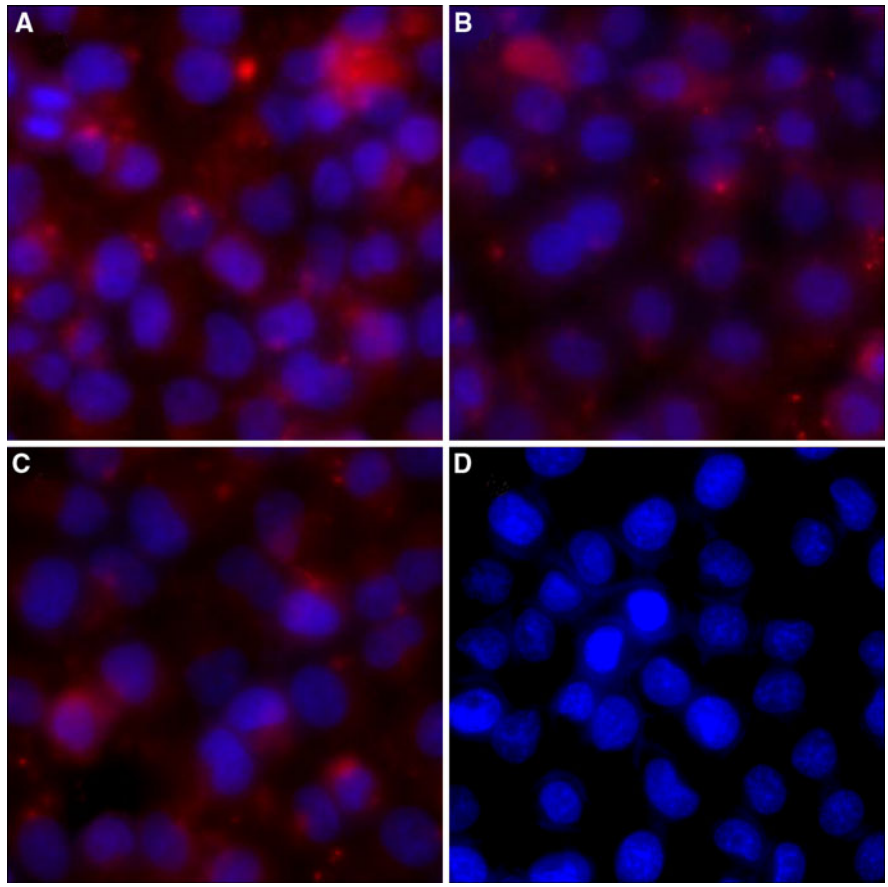

Fig. 11 **a** HeLa cells treated with SPION-NH_2 after 4 h incubation. **b** HeLa cells treated with SPION-SH after 4 h incubation. **c** HeLa cells treated with SPION-COOH after 4 h incubation. **d** Control HeLa cells with similar concentration

in vitro biocompatibility, cell uptake, and MR imaging studies. All these positive attributes make these functional SPIONs a promising platform for detection and diagnostics.

Acknowledgments The authors gratefully acknowledge IIT Kharagpur and CSIR, New Delhi for providing financial support for this work.

References

Aryal S, Remant BKC, Dharmaraj N, Bhattarai N, Kim CH, Kim HY (2006) Spectroscopic identification of S-Au interaction in cysteine capped gold nanoparticles. Spectrochim Acta A 63:160–163

Bee A, Massart R, Neveu S (1995) Synthesis of very fine maghemite particles. J Magn Magn Mater 149:6–9

Bulte JWM, Kraitchman DL (2004) Iron oxide MR contrast agents for molecular and cellular imaging. NMR Biomed 17:484–499

Chang YC, Chen DH (2005) Adsorption kinetics and thermodynamics of acid dyes on a carboxymethylated chitosan-conjugated magnetic nano-adsorbent. Macromol Biosci 5:254–261

Chen ZP, Xu RZ, Zhang Y, Gu N (2008) Effects of proteins from culture medium on surface property of silanes-functionalized magnetic nanoparticles. Nanoscale Res Lett 4:204–209

Chithrani BD, Ghazani AA, Chan WCW (2006) Determining the size, shape dependence of gold nanoparticle uptake into mammalian cells. Nano Lett 6:662–668

Das M, Mishra D, Maiti TK, Basak A, Pramanik P (2008) Bio-functionalization of magnetite nanoparticles using an aminophosphonic acid coupling agent: new, ultradispersed, iron-oxide folate nanoconjugates for cancer-specific targeting. Nanotechnology 19:415101–415115

Das M, Dhak P, Gupta S, Mishra D, Maiti TK, Basak A, Pramanik P (2010) Highly biocompatible and water-dispersible, amine functionalized magnetite nanoparticles, prepared by a low temperature, air-assisted polyol process: a new platform for bio-separation and diagnostics. Nanotechnology 21:125103–125115

Dilnawaz F, Singh A, Mohanty C, Sahoo SK (2010) Dual drug loaded superparamagnetic iron oxide nanoparticles for targeted cancer therapy. Biomaterials 31:3694–3706

Flory PJ (1953) Principles of polymer chemistry. Cornell University Press, Ithaca, NY

Gu H, Xu K, Xu C, Xu B (2006) Biofunctional magnetic nanoparticles for protein separation and pathogen detection. Chem Commun 941–949

Hong RY, Feng B, Chen LL, Liu GH, Li HZ, Zheng Y, Wei DG (2008) Synthesis characterization, MRI application of dextran-coated Fe_3O_4 magnetic nanoparticles. Biochem Eng J 42:290–300

Hu F, Wei L, Zhou Z, Ran Y, Li Z, Gao M (2006) Preparation of biocompatible magnetite nanocrystals for in vivo magnetic resonance detection of cancer. Adv. Mater 18:2553–2556

Huang HC, Chang PY, Chang K, Chen CY, Lin CW, Chen JH, Mou CY (2009) Formulation of novel lipid-coated magnetic nanoparticles as the probe for in vivo imaging. J Biomed Sci 16:86

Jun YW, Lee JH, Cheon J (2008) Chemical design of nanoparticle probes for high-performance magnetic resonance imaging. Angew Chem Int Ed 47:5122–5135

Kast CE, Schnürch AB (2001) Thiolated polymers-thiomers: development, in vitro evaluation of chitosan–thioglycolic acid conjugates. Biomaterials 22:2345–2352

Kawaguchi T, Hanaichi T, Hasegawa M, Maruno S (2001) Dextran-magnetite complex: conformation of dextran chains, stability of solution. J Mater Sci Mater Med 12:121–127

Kim EH, Lee HS, Kwak BK, Kim BK (2005) Synthesis of ferrofluid with magnetic nanoparticles by sonochemical method for MRI contrast agent. J Magn Magn Mater 289:328–330

Lee HS, Kim EH, Shao HP, Kwak BK (2005) Synthesis of spio-chitosan microspheres for MRI-detectable embolotherapy. J Magn Magn Mater 293:102–105

Levy FE, Andry MC, Levy MC (1993) Determination of free amino group content of serum albumin microcapsules using trinitrobenzenesulfonic acid: effect of variations in polycondensation pH. Int J Pharm 96:85–90

Li GY, Jiang YR, Huang Kl, Ding P, Chen J (2008) Preparation, properties of magnetic Fe_3O_4–chitosan nanoparticles. J Alloys Compd 466:451–456

Lin H, Watanabe Y, Kimura M, Hanabusa K, Shirai H (2003) Preparation of magnetic poly(vinyl alcohol) (PVA) materials by in situ synthesis of magnetite in a PVA matrix. J Appl Polym Sci 87:1239–1247

Lin JJ, Chen JS, Huang SJ, Ko JH, Wang YM, Chen TL, Wang LF (2009) Folic acid–Pluronic F127 magnetic nanoparticle clusters for combined targeting, diagnosis, and therapy applications. Biomaterials 30:5114–5124

Ma Hl, Qi Xr, Maitani Y, Nagai T (2007) Preparation and characterization of superparamagnetic iron oxide nanoparticles stabilized by alginate. Int J Pharm 333:177–186

Marco MD, Guilbert I, Port M, Robic C, Couvreur P, Dubernet C (2007) Colloidal stability of ultrasmall superparamagnetic iron oxide (USPIO) particles with different coatings. Int J Pharm 331:197–203

Mohapatra S, Pramanik P (2009) Synthesis and stability of functionalized iron oxide nanoparticles using organophosphorus coupling agents. Colloids Surf A 339:35–42

Nath S, Kaittanis C, Vasanth R, Dalal NS, Perez JM (2009) Synthesis, magnetic characterization, and sensing applications of novel dextran-coated iron oxide nanorods. Chem Mater 21:1761–1767

Petri-Fink A, Steitz B, Finka A, Salaklang J, Hofmann H (2008) Effect of cell media on polymer coated superparamagnetic iron oxide nanoparticles (SPIONs): colloidal stability, cytotoxicity, and cellular uptake studies. Eur J Pharmacol Biopharm 68:129–137

Ravi Kumar MNV, Muzzarelli RAA, Muzzarelli C, Sashiwa H, Domb AJ (2004) Chitosan chemistry and pharmaceutical perspectives. Chem Rev 104:6017–6084

Schnürch AB, Scholler S, Biebel RG (2000) Development of controlled drug release systems based on thiolated polymers. J Control Release 66:39–48

Schnürch AB, Hornof M, Guggi D (2004) Thiolated chitosans. Eur J Pharmacol Biopharm 57:9–17

Shen T, Weissleder R, Papisov M, Bogdanov A, Brady TJ (1993) Monocrystalline iron-oxide nanocompounds (MION) physicochemical properties. Magn Reson Med 29:599–604

Shi XY, Wang SH, Swanson SD, Ge S, Cao ZY, Van Antwerp ME, Landmark KJ, Baker JR (2008) Dendrimer-functionalized shell-crosslinked iron oxide nanoparticles for in vivo magnetic resonance imaging of tumors. Adv Mater 20:1671–1678

Smaihi M, Gavilan E, Durand J, Valtchev VP (2004) Colloidal functionalized calcined zeolite nanocrystals. J Mater Chem 14:1347–1351

Sonvico F, Mornet S, Vasseur S, Dubernet C, Jaillard D, Degrouard J, Hoebeke J, Duguet E, Colombo P, Couvreur P (2005) Folate-conjugated iron oxide nanoparticles for solid tumor targeting as potential specific magnetic hyperthermia mediators: synthesis, physicochemical characterization, and in vitro experiments. Bioconjugate Chem 16:1181–1188

Tan H, Xue JM, Shuter B, Li X, Wang J (2010) Synthesis of PEOlated Fe_3O_4@SiO_2 nanoparticles via bioinspired silification for magnetic resonance imaging. Adv Funct Mater 20:722–731

Veiseh O, Sun C, Gunn J, Kohler N, Gabikian P, Lee D, Bhattarai N, Ellenbogen R, Sze R, Hallahan A, Olson J, Zhang M (2005) Optical and MRI multifunctional nanoprobe for targeting gliomas. Nano Lett 5:1003–1008

Wang S, Zhou Y, Yang S, Ding B (2008) Growing hyperbranched polyglycerols on magnetic nanoparticles to resist nonspecific adsorption of proteins. Colloids Surf B 67:122–126

Weissleder R, Bogdanov A, Neuwelt EA, Papisov M (1995) Long-circulating iron oxides for MR imaging. Adv Drug Delivery Rev 16:321–334

Weissleder R, Moore A, Mahmood U, Bhorade R, Benveniste H, Chiocca EA, Basilion JP (2000) In vivo magnetic resonance imaging of transgene expression. Nat Med 6:351–354

Win KY, Feng S (2005) Effects of particle size, surface coating on cellular uptake of polymeric nanoparticles for oral delivery of anticancer drugs. Biomaterials 26:2713–2722

Yi H, Wu LQ, Bentley WE, Ghodssi R, Rubloff GW, Culver JN, Payne GF (2005) Biofabrication with chitosan. Biomacromolecules 6(6):2881–2894

Yin L, Ding J, He C, Cui L, Tang C, Yin C (2009) Drug permeability, mucoadhesion properties of thiolated trimethyl chitosan nanoparticles in oral insulin delivery. Biomaterials 30:5691–5700

Yuan JJ, Armes SP, Takabayashi Y, Prassides KC, Galembeck F, Lewis AL (2006) Synthesis of biocompatible poly[2-(methacryloyloxy)ethyl phosphorylcholine]-coated magnetite nanoparticles. Langmuir 22:10989–10993

Zhang Y, Kohler N, Zhang M (2002) Surface modification of superparamagnetic magnetite nanoparticles and their intracellular uptake. Biomaterials 23:1553–1561

Zhu A, Yuan L, Liao T (2008) Suspension of Fe_3O_4 nanoparticles stabilized by chitosan, o-carboxymethylchitosan. Int J Pharm 350:361–368